

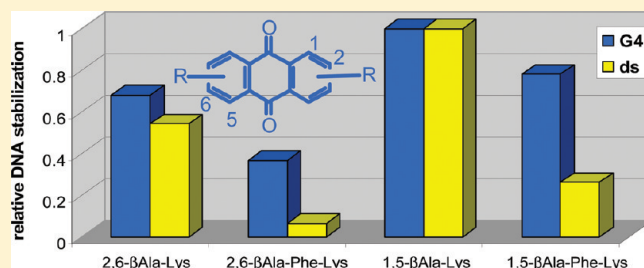
Tuning G-Quadruplex vs Double-Stranded DNA Recognition in Regioisomeric Lysyl-Peptidyl-Anthraquinone Conjugates

Giuseppe Zagotto, Antonio Ricci, Elena Vasquez, Andrea Sandoli, Silvia Benedetti, Manlio Palumbo, and Claudia Sissi*

Department of Pharmaceutical Sciences, University of Padova, Via Marzolo 5, 35131 Padova, Italy

S Supporting Information

ABSTRACT: Anthraquinone is a versatile scaffold to provide effective DNA binders. This planar system can be easily conjugated to protonable side chains: the nature of the lateral groups and their positions around the tricyclic moiety largely affect the DNA recognition process in terms of binding affinity and mode, as well as sequence and structure of the target nucleic acid. Starting from an anthracenedione system symmetrically functionalized with N-terminal lysyl residues, we incremented the length of side chains by introducing a Gly, Ala, or Phe spacer, characterized by different flexibility, lipophilicity, and bulkiness. Moreover, 2,6, 2,7, 1,8, and 1,5 regioisomers were examined to yield a small bis(lysyl-peptidyl) anthracenedione library. By merging spectroscopic, enzymatic, and cellular results, we showed that the proper combination of a basic aminoacid (Lys) with a more hydrophobic residue (Phe) can provide selective G-quadruplex recognition, in particular when side chains are located at positions 2,6 or 2,7. In fact, while these derivatives effectively bind G-quadruplex structures, they behave at the same time as rather poor double-stranded DNA intercalators. As a result, the Lys-Phe substituted anthraquinones are poorly cytotoxic but still able to promote a senescence mechanism in cancer cells. This combination of chemical and biological properties foresees potentially valuable applications in anticancer medicinal chemistry.



INTRODUCTION

Telomeres are specialized nucleoprotein structures localized at the end of chromosomes. They protect genomic information from degradation, fusion, and recombination and allow the DNA damage response machinery to discriminate between double-strand breaks and natural chromosome ends.¹ Telomeric DNA comprises several kilobases of tandem repeats of a G-rich DNA sequence (TTAGGG in humans) and are characterized by a single-stranded 3' end (ca. 150–200 nucleotides). However, its length is progressively reduced in somatic cells due to the “end replication” problem.² When telomeres reach a critical length, cells enter a replicative senescence state and division no longer occurs.³ On the contrary, over 80% of cancer cells maintain telomere integrity due to an up-regulation of a reverse transcriptase called telomerase.⁴ This enzyme catalyzes the synthesis of telomeric DNA repeats, stabilizing telomeres length and contributing to cellular immortalization and oncogenesis.⁵

Due to its involvement in cell immortalization, telomerase represents a promising anticancer target.⁶ Various strategies have been devised to directly target the enzyme or associated proteins. An alternative approach comprises derivatives directed toward the 3' single-stranded end of telomeric DNA.⁷ In this case, small molecules are used to induce nucleic acid folding into a noncanonical structure called the G-quadruplex,

which is inaccessible to the RNA template component of telomerase.⁸

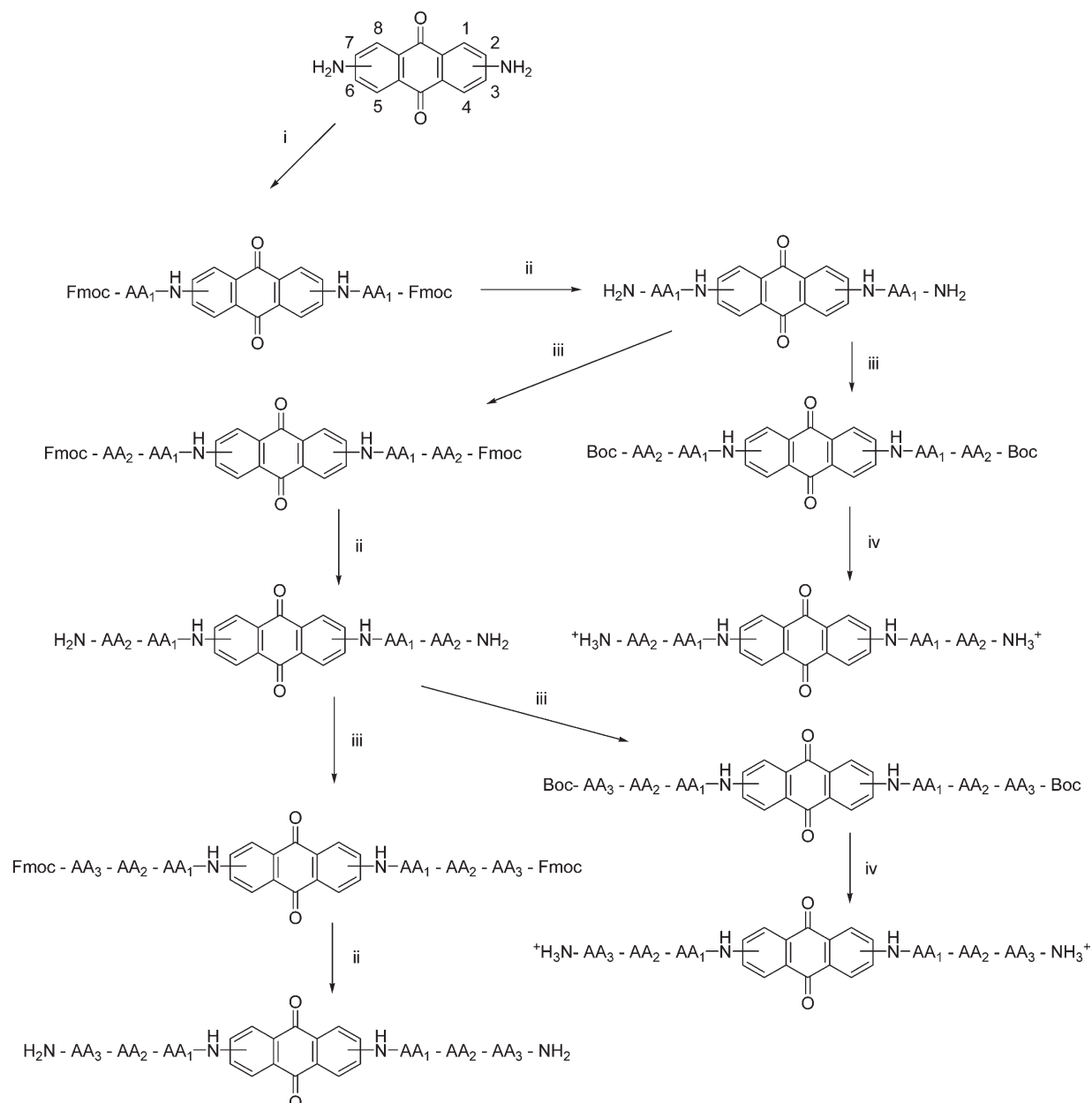
In the past decades, a large number of small molecules have been reported to efficiently bind G-quadruplex DNA and to inhibit telomerase.^{9–11} Most of them are based on a polycyclic aromatic core that stacks by π – π interactions over the terminal planar G-tetrads of a quadruplex. In addition, cationic side chains can interact with the negatively charged phosphate backbones in G-quadruplexes.

Properly substituted anthraquinones were early identified as potential effective G-quadruplex binders.^{12–14} In particular, the substitution pattern with protonable side chains was shown to play a major role in driving selectivity toward double-stranded or G-quadruplex structures. In previous studies, we reported the modulation of G-quadruplex recognition by anthracenedione derivatives symmetrically disubstituted at 2,6 or 2,7 positions with one or two aminoacidic residues.^{15,16} We showed the importance of the size of the planar surface, which was affected by reversal of the direction of the amide linkage connecting the anthracenedione to the side chains. Additionally, a significant role of ionic interactions was confirmed, since N-terminal protonable

Received: July 19, 2011

Revised: August 26, 2011

Published: September 12, 2011

Scheme 1^a

^a Reagents: (i) AA₁-Cl, DMF, RT, N₂, 3 h. (ii) Piperidine/DMF 20%, RT, 20 min. (iii) AA_{2,3,4}, TBTU, HOBT, DIPEA, RT, N₂, DMF, 4 h. (iv) TFA/H₂O 90%, RT, 20 min.

was repeated at least three times and errors were ± 0.4 °C. ΔT_m were calculated by subtracting the T_m value recorded in the presence of the ligand from the corresponding value in the absence of ligand.

Circular Dichroism Measurements. Circular dichroism spectra from 220 to 450 nm were recorded using 10 mm path length cells on a Jasco J 810 spectropolarimeter equipped with a NESLAB temperature controller and interfaced to a PC 100 in 10 mM Tris-HCl, 50 mM KCl pH 7.4. Before data acquisition, Tel22 solutions (4 μ M) were heated at 95 °C for 5 min and left to cool overnight at room temperature. The reported spectrum of each sample represents the average of 3 scans recorded with 1 nm step resolution. Observed ellipticities were

converted to mean residue ellipticity $[\theta] = \text{deg} \times \text{cm}^2 \times \text{d mol}^{-1}$ (Mol. Ellip.).

Electromobility Shift Assay. End-labeled single-stranded oligonucleotides were obtained by incubating the oligonucleotides with T4 polynucleotide Kinase and [γ -³²P] ATP for 30 min at 37 °C. The enzyme was then removed by extraction with phenol/chloroform/isoamyl alcohol (25:24:1). A mixture of purified labeled and unlabeled oligonucleotides (total final concentration 10 μ M) was heated to 95 °C for 5 min in 10 mM Tris, 1 mM EDTA, 100 mM KCl, pH 8.0 buffer and allowed to cool overnight at room temperature. The folding of the starting material was monitored by native 16% polyacrylamide gel electrophoresis in 0.5 \times TBE (44.5 mM Tris base, 44.5 mM boric

acid and 1 mM Na₂EDTA) added of KCl (100 mM in buffer and 20 mM in gels).

Resolved bands on dried gels were visualized and quantified on a PhosphorImager (Amersham).

Taq Polymerase Assay. Compounds were assayed with *Taq* polymerase reaction by using pBR322 (2.5 ng) as DNA template and appropriate primer sequences (T_{up} and T_{down} , 0.5 μ M each) to amplify the 964–1064 plasmid sequence by PCR. The reaction was carried out in a Perkin-Elmer thermocycler performing 25 cycles of 30 s at 94 °C, 30 s at 65 °C, and 30 s at 72 °C. The reaction products were resolved on a 2% agarose gel in 1 \times TBE (89 mM Tris base, 89 mM boric acid, and 2 mM Na₂EDTA) and stained by ethidium bromide.

Telomerase Activity Assay (TRAP Assay). Telomerase activity was assayed using a modified telomere repeat amplification protocol (TRAP) assay. As a source of telomerase, the total cell lysates derived from human melanoma cell line HeLa were used. Protein concentration of the lysates was assayed using Bio-Rad protein assay kit using BSA as standard. A 50 μ L TRAP reaction mix (50 μ M of dNTPs, 0.2 μ g of primer TS, 0.1 μ g of return primer ACX, 500 ng of protein extract, 2 U *Taq* polymerase) was prepared in the presence/absence of increasing drug concentration in 20 mM Tris-HCl, pH 8.3, 68 mM KCl, 1.5 mM MgCl₂, 1 mM EGTA, 0.05% v/v Tween-20. An internal control template (0.01 mmol TSNT) with its return primer (1 ng NT) were added to the reaction mixture. Then, the telomerase elongation step has been performed (30 min at 30 °C) followed by a PCR amplification step (30 cycles of 30 s at 37 °C and 30 s at 58 °C). Telomerase products were resolved by 10% polyacrylamide gel electrophoresis in TBE 0.5 \times and visualized by staining with Sybr Green I.

MTT Assays. HeLa (human hepitelial) cell line was maintained in DMEM medium supplemented with 10% heat-inactivated fetal calf serum, 50 U/mL of penicillin G, and 50 μ g/mL of streptomycin, at 37 °C in humidified atmosphere and 5% of CO₂.

To evaluate toxic profiles of the potential antitelomerase compounds, MTT assays were performed as described: cells were plated in 96 well plates at 10 000 cells/well, and cultured overnight. Afterward, compounds were added in triplicate and plates were incubated in the presence of the drug for 72 h. At the end of this period, MTT was added to a final concentration of 0.8 mg/mL, and two additional hours of incubation were performed. After that, medium was aspirated carefully and 150 μ L of DMSO were added per well. Soluble formazan salts were homogenized by manual pipetting and absorbance at 540 nm was read. Curves consisted of 8 serial dilutions in triplicate in each case, and results were analyzed as sigmoidal dose–response curves.

Cell Senescence Assay. HeLa cells were plated in 6-well plates at 10 000 cells/well and cultured overnight. Afterward, compounds were added in triplicate (2.5 μ M and 0.5 μ M for C-16 and D-16, respectively) and plates were incubated in the presence of the drug for 240 h. Every 72 h, the medium was changed and new drug was added. At the end of the treatment, medium was removed and cells were washed once with 1 mL of PBS and fixed with 1 mL of 2% formaldehyde, 0.2% glutaraldehyde in PBS for 15 min at room temperature. After another washing step with PBS, cells were stained with 1 mL of 37.2 mM citric acid/sodium phosphate (pH 6.0), 140 mM NaCl, 1.8 mM MgCl₂, 5 mM K₃Fe(CN)₆, 5 mM K₄Fe(CN)₆ 3H₂O, and 1 mg/mL X-gal in dimethylformamide. Plates were incubated overnight at 37 °C and then photographed with a light microscope.

Scheme 2

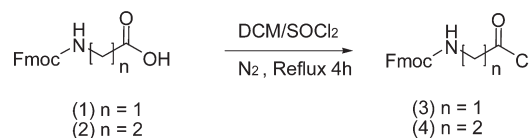


Table 1. Schematic Structures of the Synthesized 9,10-Anthracenedione-Aminoacyl Conjugates

regioisomer	compound	side chains		
		AA ₁	AA ₂	AA ₃
2,6	A-13	Gly	Lys	
	A-14	Gly	Ala	Lys
	A-15	Gly	Gly	Lys
	A-16	Gly	Phe	Lys
2,6	B-13	β Ala	Lys	
	B-14	β Ala	Ala	Lys
	B-15	β Ala	Gly	Lys
	B-16	β Ala	Phe	Lys
2,7	C-13	β Ala	Lys	
	C-14	β Ala	Ala	Lys
	C-16	β Ala	Phe	Lys
1,5	D-13	β Ala	Lys	
	D-14	β Ala	Ala	Lys
	D-16	β Ala	Phe	Lys
1,8	E-13	β Ala	Lys	
	E-14	β Ala	Ala	Lys
	E-16	β Ala	Phe	Lys

RESULTS

Chemistry. Starting materials for the synthesis of all derivatives were the appropriate diamino-substituted anthraquinones (AQ). While 2,6-diamino and 1,5-diamino AQ are commercially available, the 2,7-diamino and 1,8-diamino AQ were obtained via reduction of the corresponding dinitro derivatives.¹⁷ In particular, the 2,7-dinitro AQ scaffold was obtained through a one-pot nitration–oxidation of commercial anthrone, as previously described.¹⁶ The common synthetic route for all the disubstituted AQs is summarized in Scheme 1. Due to the low reactivity of the aryl amino groups, the first aminoacidic coupling (AA1) was efficiently carried out using the appropriate acyl chloride derivative (AA-Cl). These substrates were prepared treating the selected AA (Fmoc-glycine or Fmoc- β -alanine) with an excess of thionyl chloride in CH₂Cl₂ (Scheme 2). A first Fmoc deprotection of the amino groups, followed by salification with trifluoroacetic acid (TFA) led to the first group of compounds (A-2, B-2, C-2, D-2, and E-2). The salification step was performed to favor the solubility of the anthraquinone derivatives in water.

These compounds were used as starting blocks to synthesize several derivatives which can be divided into 5 related families: **A** and **B** where a glycine or a β -alanine was the AA₁ at positions 2 and 6, respectively; **C**, **D**, and **E** which correspond to the 2,7, 1,5, and 1,8 regioisomers of compound **B**.

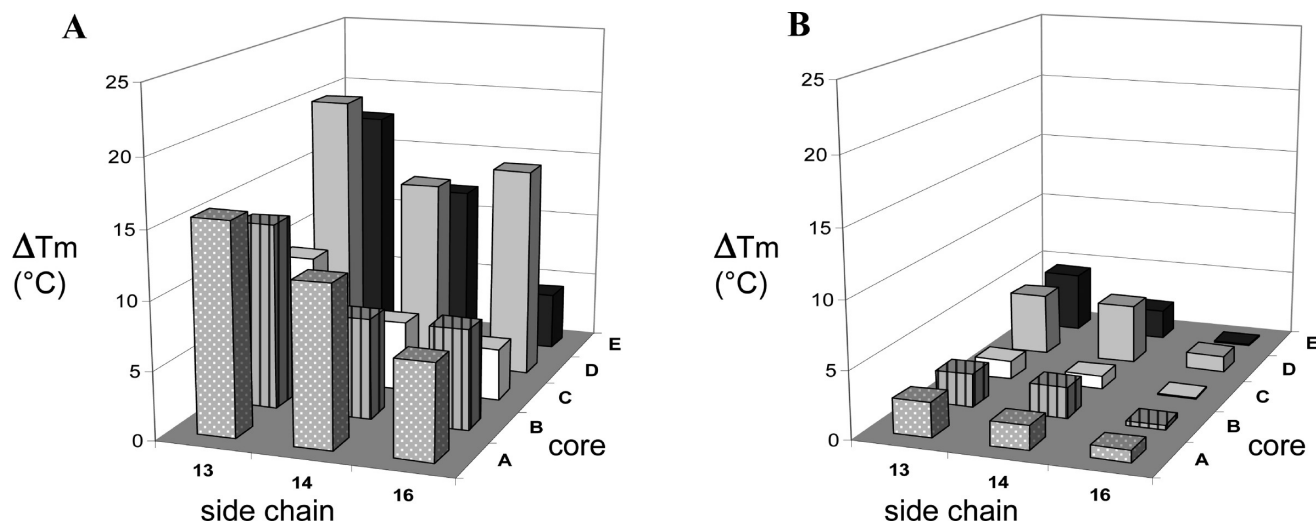


Figure 1. Variation of the melting temperature (ΔT_m) of a G-quadruplex folded telomeric sequence (A, $0.25 \mu\text{M}$) or double-stranded DNA (B, $0.25 \mu\text{M}$) upon addition of $1 \mu\text{M}$ selected anthraquinones in 50 mM KCl . Errors were $\pm 0.4 \text{ }^\circ\text{C}$.

The novel derivatives were prepared by standard peptide coupling of the free amino $\text{AA}_1\text{-AQ}$ and the desired Fmoc- or Boc-protected AA_2 derivatives using TBTU, HOBt, and DIPEA as coupling reagents (Scheme 2). In the first case, basic deprotection led to the free amino derivatives, which were coupled with a third amino acid or salfied with TFA to afford more water-soluble derivatives. In the case of the Boc-protected compounds, the acidic condition used to remove the Boc protective group directly led the desired trifluoroacetic salts derivatives. The side chains composition of the synthesized anthraquinones is reported in Table 1.

Fluorescence Melting Assays. All test derivatives were evaluated for their ability to bind and stabilize G-quadruplex structures by fluorescence melting measurements.

We used an oligonucleotide corresponding to the human telomeric sequence labeled at the $5'$ -end with a quencher (dabcyl) and at the $3'$ -end with a fluorophore (fluorescein). When the oligonucleotide folds into an intramolecular G-quadruplex, these groups are in close proximity, and as a consequence, the fluorescence is quenched. When DNA melts, the strands fall far apart and a large increase in fluorescence occurs. This system allows us to easily monitor DNA folding/unfolding processes upon temperature variation.^{18,19} Drug binding to DNA affects nucleic acid stability, hence its melting temperature (T_m). Since a correlation exists between the observed T_m shift (ΔT_m) and the DNA binding affinity of structurally related binders, this allows us to build a relative G-quadruplex affinity ranking order.²⁰ Thus, the melting profile of the oligonucleotide (T_m in the absence of ligand $57.2 \text{ }^\circ\text{C}$) was recorded in the presence of increasing anthracenedione concentration ($0\text{--}20 \mu\text{M}$, Supporting Information). The ΔT_m values determined for all derivatives at $1 \mu\text{M}$ concentration are included in Table 3. The behavior of the test ligands toward telomeric G-quadruplex is generally conserved among the 5 tested families (Figure 1A). In particular, it emerged that the introduction of an amino acid between AA_1 and the charged residue sensibly reduces the G-quadruplex stabilizing efficiency. This effect is more significant when shifting from Gly or Ala to become maximal with Phe. This suggests that the flexibility and bulkiness of the linker is relevant for G-quadruplex interaction, likely favoring the proper localization of the positive charge on the polyanionic target.

Fluorescence melting analysis was used also to evaluate the preference of the new derivatives for G-quadruplex structure vs duplex DNA arrangement by using a random double-stranded sequence ($5'$ -GTGAGATACCGACAGAAG, T_m $52.8 \text{ }^\circ\text{C}$). The ΔT_m value determined for all derivatives at $1 \mu\text{M}$ concentration are included in Table 3 and plotted in Figure 1B. All tested compounds stabilize double-stranded DNA to a considerably lesser extent than G-quadruplex. Interestingly, dsDNA recognition is more prominent for derivatives of the D and E families that bear substituents at positions 1,5 or 1,8. Comparison of melting data on different DNA folding underlines that for derivatives containing the Phe-Lys dipeptide (compounds with side chain -16) relevant thermal stabilization occurs only with the G-quadruplex structure, which suggests remarkable selectivity in the drug–DNA recognition process.

For a direct comparison of the ligand-mediated DNA stabilization on the two tested folds, melting profiles of the telomeric sequence were recorded in the presence of variable amounts of its complementary strand (Figure 2).²¹ The results confirmed that the Phe-Lys containing analogues are the most selective for G-quadruplex structures. Indeed, they are the only derivatives able to increment the melting temperature of the quadruplex form when the double-stranded arrangement is highly favored (presence of an excess of complementary C-rich strand).

Circular Dichroism. The peculiar signature of the CD spectrum of the G-quadruplex folded telomeric sequence Tel22 is well-characterized. In potassium-containing buffer, it shows a positive band at 295 nm with a shoulder at 260 nm , which corresponds to a mixed type (antiparallel and parallel) strand arrangement.²² Tel22 dichroic response was extensively modified in the presence of increasing concentrations of our ligands, thus confirming that they are effective binders (Figure 3). In particular, CD titrations confirmed a strong binding affinity for all tested compounds to G-quadruplex: saturation occurred at comparable drug/DNA ratio and indicated the binding of two anthraquinones per G-quadruplex unit (Figure 3C). In analogy to most of the known G-quadruplex interacting agents, this supports the stacking of one ligand on both terminal tetrads of the G-quadruplex.

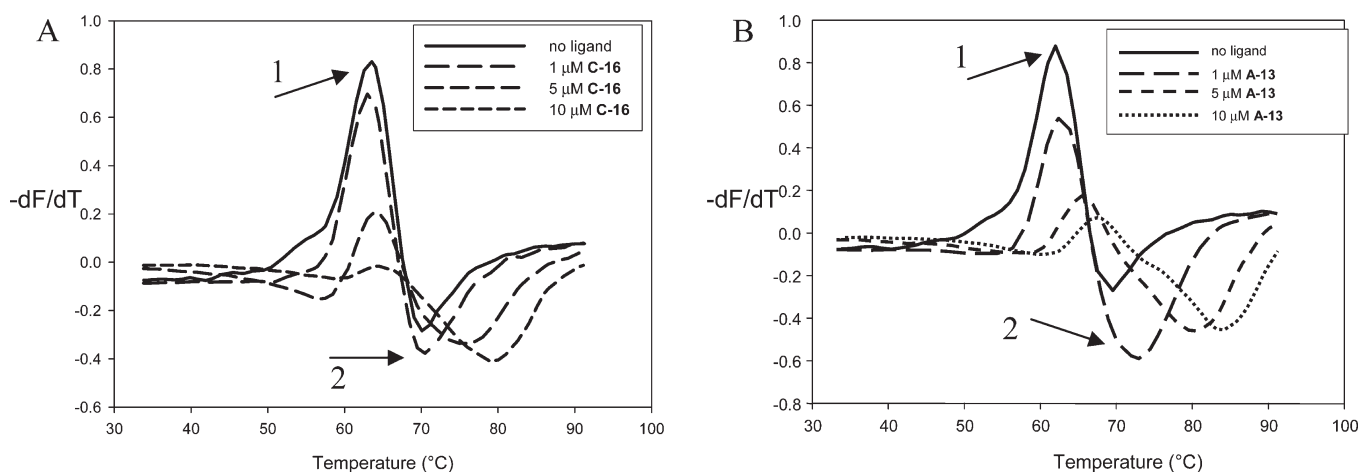


Figure 2. First derivatives of the melting profiles of a G-quadruplex folded telomeric sequence ($0.25 \mu\text{M}$) recorded in the presence of an excess (20-fold) of its complementary strand in 50 mM KCl. Arrows 1 and 2 indicate the shifts of the duplex and quadruplex melting transitions, respectively. Panels A and B refer to addition of C-16 and A-13, respectively.

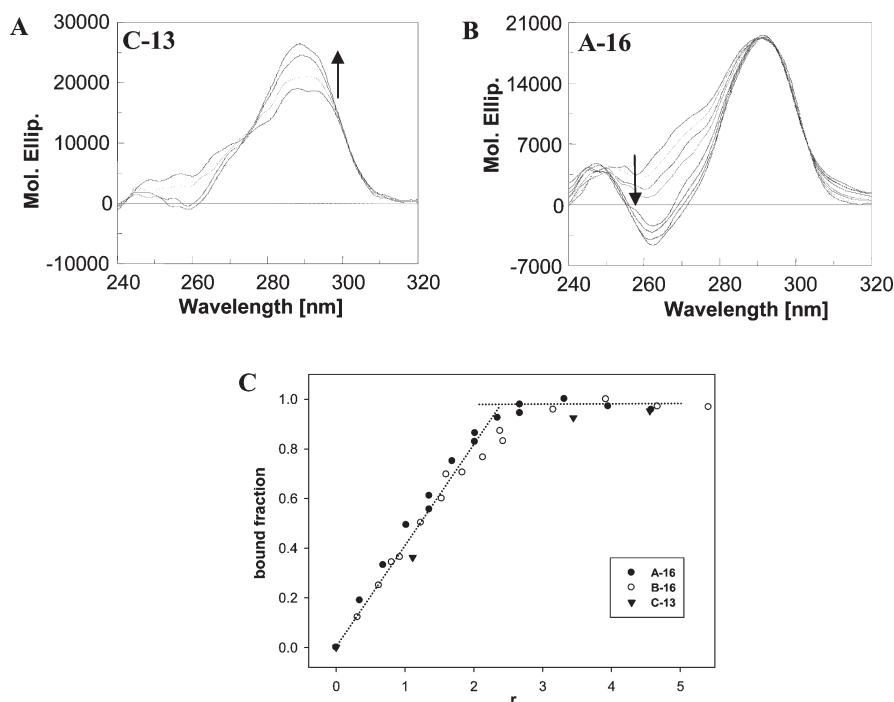


Figure 3. Circular dichroism spectra of Tel22 ($4 \mu\text{M}$) recorded in the presence/absence of anthraquinone derivatives in 10 mM Tris, 50 mM KCl, pH 7.4, 25 °C. Arrows indicate the changes induced by increasing concentrations of C-13 (A) and A-16 (B). The variation of the fraction of bound Tel22 upon increasing ligand/DNA ratio (r) determined by CD titrations is described in panel C.

Generally, an increment in the positive band at 295 nm is observed suggesting a stabilization of the antiparallel components of the G-quadruplex nucleic acid structure. Interestingly, the Phe-Lys substituted derivatives (compounds with side chain -16) induced the most notable variations at 260 nm. Since the tested derivatives showed comparable absorption spectra and, additionally, no significant induced CD in the drug absorption range, we are confident in assigning the observed differences primarily to slightly different binding modes.

When similar measurements were performed using a double-stranded DNA (we used calf thymus DNA, ctDNA, due to its similarity to the human nucleic acid composition) as the target,

we still found odd behaviors for derivatives containing the Phe-Lys sequence (Figure 4B). In general (see, for example, the series -13, Figure 4A), an increment of the DNA dichroic intensity at 275 nm occurred which sustains intercalation into the double helix. On the contrary, all Phe-Lys containing derivatives showed a reduction in the DNA band intensities at both 275 and 245 nm (Figure 4B). Although this confirms a DNA–ligand interaction, it suggests that intercalation is probably not the principal binding mechanism. Generally, DNA intercalation of anthraquinone derivatives disubstituted at positions 1,5, 2,6, and 2,7 occurs by a threading mechanism with the planar system being oriented more or less perpendicularly to the base pair longest dimension

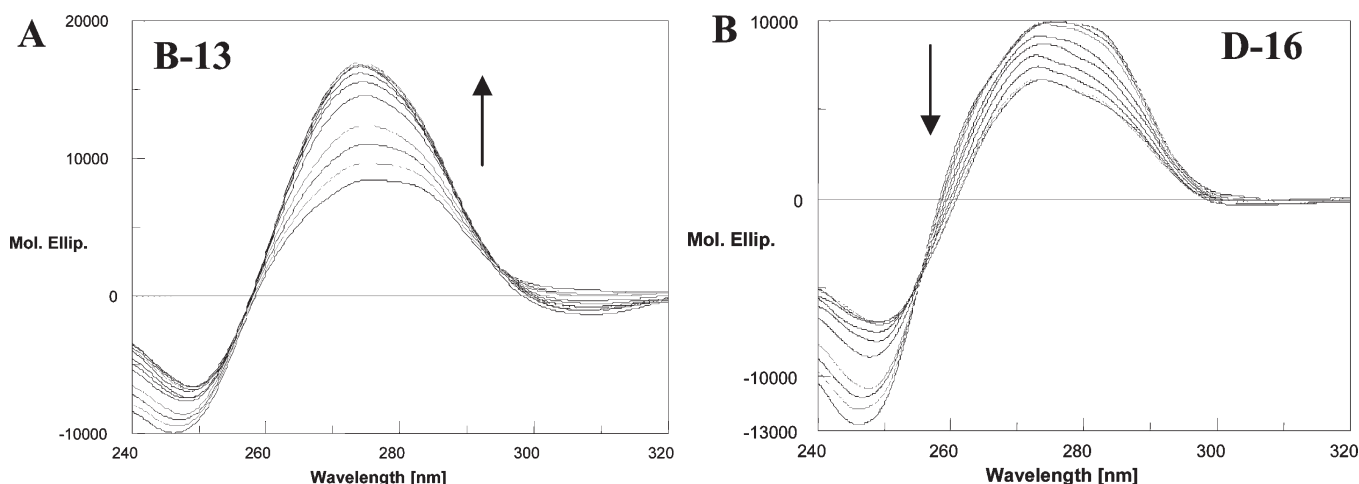


Figure 4. Circular dichroism spectra of ctDNA ($88 \mu\text{M}$) recorded in the presence of increasing concentrations of anthraquinone derivatives in 10 mM Tris, 50 mM KCl, pH 7.4, 25°C .

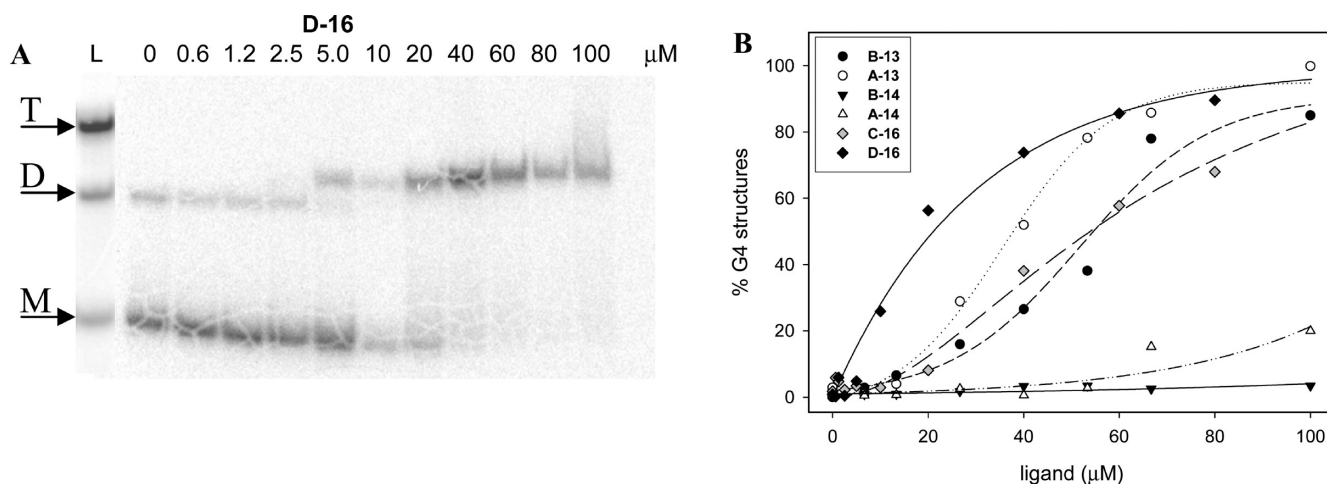


Figure 5. Induction of G-quadruplex structure by selected ligands in 10 mM Tris, 50 mM KCl, pH 7.4, 25°C . Panel A: variation of the electrophoretic mobility of the unfolded oligonucleotide 2GGG ($10 \mu\text{M}$) upon addition of D-16 due to its conversion into a dimeric G-quadruplex. A marker (L) for the monomeric (M), dimeric (D), or tetrameric (T) form is included. Panel B: plot of % of G-quadruplex forms promoted by increasing ligands concentrations.

and one side chain located in each DNA groove.²³ We can infer that the presence of the bulky Phe residue prevents threading of the side chains between the base pairs. As a result, an external binding mode promoted by the presence of highly charged residues in the side chains can be favored. This is particularly true for B-16, since it converts dsDNA into an insoluble compact form also at low ligand/DNA ratio.

Electromobility Shift Assay. Electromobility shift assays were performed to evaluate the ability of tested molecules to induce G-quadruplex folding of the human telomeric sequence (Figure 5).

In these experiments, we used an oligonucleotide which contains two repeats of the human telomeric sequence TTAGGG (2GGG). This sequence can form intermolecular (dimeric or tetrameric) G-quadruplex structures that migrate more slowly than the nonstructured single-stranded DNA (Figure 5A). None of our tested derivatives promoted the formation of tetrameric G-quadruplexes. However, some of them were able to promote induction of a dimeric G-quadruplex arrangement of the 2GGG sequence depending upon side chain composition.

Negligible conversion of oligomer 2GGG to an intermolecular G-quadruplex structure was observed when an amino acid is interposed between the AA₁ and the N-terminal Lys residue (compare compounds -13 with homologues -14; Figure 5B). Interestingly, the presence of a Phe (compounds with side chain -16) that was observed to comparably reduce the thermal stability of the DNA–ligand complex, allows retention of effective G-quadruplex induction, the most successful being derivative D-16 with side chains located at positions 1,5. These data further support a peculiar behavior associated to the presence of a Phe residue in the side chains.

Enzymatic Inhibition and Cell Toxicity Assays. To assess possible interference of test drugs with enzymatic processes involving DNA, we examined the effects of peptidyl anthraquinones upon DNA amplification and elongation mediated by *Taq* polymerase and telomerase, respectively. In addition, we determined the cytotoxic activity of our compounds by MTT assay on HeLa human cancer cells. The results are summarized in Table 2.

Table 2. *Taq* Polymerase Inhibition, Telomerase Inhibition and Cell Cytotoxicity (MTT on HeLa cell line) Produced by the Test Anthraquinone-Aminoacyl Conjugates

compound	IC ₅₀ (μM)		
	<i>Taq</i> polymerase ^a	telomerase ^a	HeLa
A-13	5	0.8	27 ± 1.2
A-14	30	1.9	25 ± 1.5
A-15	15	0.9	57 ± 1.1
A-16	15	7.0	41 ± 1.8
B-13	10	0.8	14 ± 2.0
B-14	22	6.5	28 ± 2.7
B-15	>40	3.8	49 ± 2.3
B-16	20	7.1	57 ± 2.7
C-13	2.5	1.5	31 ± 2.6
C-14	5	3	23 ± 5.0
C-16	20	10	18 ± 3.0
D-13	2.0	n.o. ^b	2.6 ± 0.3
D-14	5	2.5	27 ± 3.3
D-16	15	4	2.5 ± 0.2
E-13	5	n.o.	1.2 ± 0.3
E-14	>40	18	1.8 ± 0.1
E-16	>40	20	6.0 ± 0.2

^a Experimental error ±4%. ^b n.o., not observed up to 40 μM.

Table 3. Increase of the Melting Temperature (Δ*T*_m °C) Produced by Tested Derivatives (1 μM) on a G-Quadruplex Folded Telomeric Sequence or Double-Stranded DNA in the Presence of 50 mM KCl^a

compound	G-quadruplex telomeric sequence	double-stranded DNA
A-13	15.6	2.6
A-14	11.9	1.8
A-15	11.0	4.0
A-16	7.1	0.9
B-13	13.7	2.5
B-14	7.4	2.3
B-15	8.2	3.6
B-16	7.4	0.3
C-13	9.5	1.4
C-14	5.2	1.0
C-16	3.9	0.1
D-13	20.1	4.6
D-14	14.1	4.5
D-16	15.7	1.2
E-13	17.6	4.5
E-14	12.1	2.2
E-16	4.3	0.1

^a DNA concentration was 0.25 μM, experimental error ±0.4°C.

For all active derivatives, inhibition of telomerase-mediated DNA elongation occurred generally at lower concentrations in comparison to DNA amplification. From these data, selective telomerase inhibition by our ligands cannot be firmly established from the present results, since competition between telomerase elongation and *Taq* polymerase amplification can occur.²⁴ In any event, the observed modulation of telomerase elongation is well-

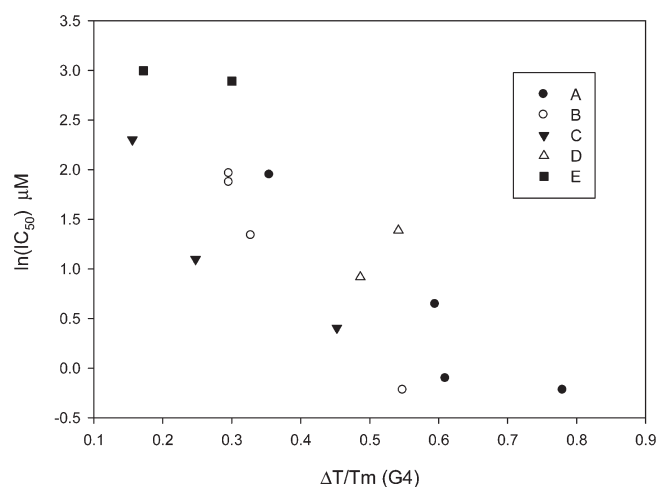


Figure 6. Correlation between Telomerase elongation inhibition (IC₅₀) and thermal stabilization (Δ*T*_m/*T*_m) of telomeric G-quadruplex measured for all tested derivatives.

related to G-quadruplex binding thermodynamics as shown by the almost linear dependence of IC₅₀ for telomerase inhibition from Δ*T*_m/*T*_m, where *T*_m is the melting temperature in the presence of saturating amounts of the drug (Figure 6).¹⁵ On the contrary, the G-quadruplex affinity data are poorly related to cell cytotoxicity.

In turn, *Taq* inhibition correlates with double-stranded DNA stabilization and, to a lesser extent, to cell cytotoxicity. In this case, the most active compounds are 1,5 and 1,8 derivatives that, indeed, were confirmed to be the most efficient DNA intercalators. We can infer that a short-term drug exposure causes an interference with processing of the nucleic acid that ultimately is translated into a cytotoxic signal.

Accordingly, poor dsDNA binders like B-16 and C-16 are poorly cytotoxic. Interestingly, however, both latter anthraquinones stimulated β-galactosidase activity in HeLa cells treated for 240 h at subcytotoxic concentrations without appreciably affecting cell growth (Figure 7), which is consistent with an induction of delayed senescence. However, when the more cytotoxic 1,5 regioisomer (D-16) was used in the same conditions, senescence induction was clearly coupled to a significant drop in cell growth. These results further emphasize the peculiar behavior of the Phe containing derivatives also at a cellular level.

DISCUSSION

The DNA binding properties of 9,10-anthracenedione derivatives have been extensively studied in the past,²⁵ highlighting that the nature of the side chains as well as their relative position are critical factors to address their DNA binding mode.^{12,14} Conceivably, the presence of positively charged groups in the side chains greatly favors the binding process although generally regardless of the sequence/structure they bind to. However, provided that different DNA arrangements locate phosphate groups at different relative distances, in principle, charged interactions could be used for selective recognition if the binders' chains are appropriately positioned with reference to the macromolecule. Here, we showed for all test derivatives that increasing the distance of the lysyl residue from the anthracenedione ring system invariably decreases G-quadruplex affinity. This is probably due to the fact that the positive charges are, on average, located more

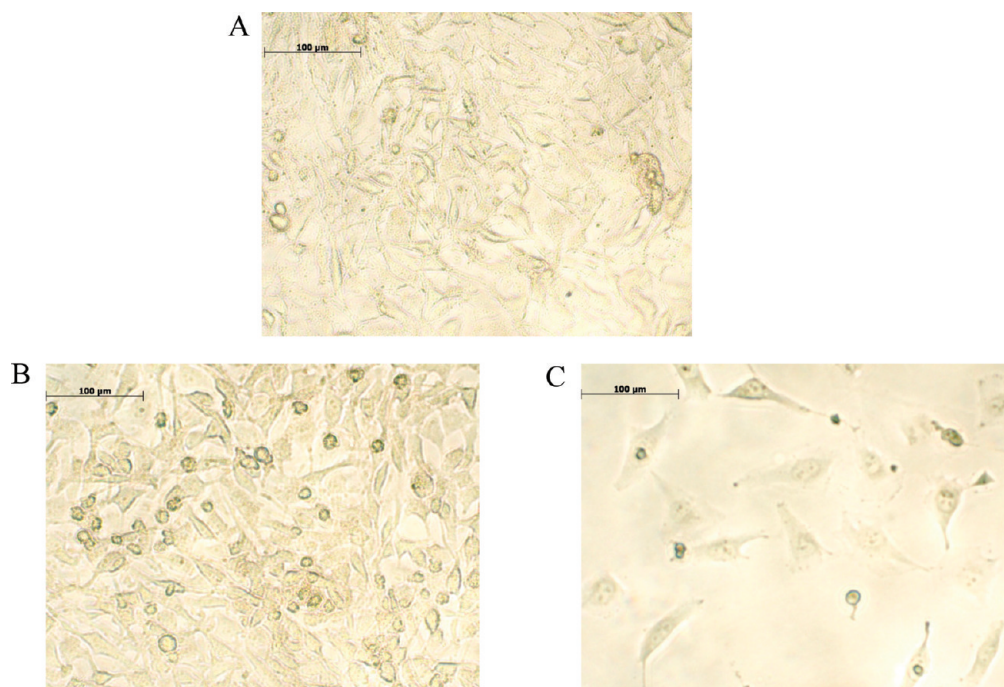


Figure 7. β -Galactosidase activity of HeLa cell when untreated (A) or treated with C-16 (B) or D-16 (C) for 144 h.

distant from the anionic sites of DNA. Hence, compounds having longer side chains with clear additional flexibility (possibly rendered less effective by the rigid peptide bonds) cannot get closer to the target counterions than the starting congeners. Apparently, introduction of the bulky Phe residue is even more detrimental than the presence of a glycine or alanine linker. However, Phe-containing derivatives turn out to be selective for G-quadruplex because, unlike other congeners, they hardly bind to double-stranded DNA, yet they are still able to stack on top of the terminal tetrads without requiring significant DNA distortion.

Shifting side chains from position 2,6 or 2,7 (families A, B, and C) to 1,5 (family D) or, to a lesser extent, to 1,8 (family E) helps increasing G-quadruplex stabilization, but at the same time, it promotes effective binding to dsDNA. Interestingly, this behavior is distinct from the one we reported for anthracene derivatives of the bisanthrene family.²⁶ In fact, among those anthracene derivatives, the shift of the side chains from 2,6 to 1,5 positions slightly incremented G-quadruplex recognition but remarkably disfavored double-stranded DNA binding. This suggests that the presence of the carbonyl groups causes different orientations of the anthracenedione vs anthracene ring when bound to G-quadruplex DNA.

As far as the biochemical and biological results, we found pronounced cell growth inhibition when the double-stranded DNA recognition process is efficient. On the other hand, the onset of senescence in cancer cells is particularly evident with the more telomerase-sensitive derivatives, which produce selective G-quadruplex stabilization. In conclusion, although we did not succeed in effectively improving G-quadruplex binding, we were able to remarkably uncouple quadruplex vs duplex affinity, which gives useful hints for future design of compounds exhibiting selectivity and efficient tetraplex-inducing properties at the same time.

■ ASSOCIATED CONTENT

S Supporting Information. Structural properties, synthetic procedures, and analytical data (NMR, HRMS, and combustion) for new compounds. This material is available free of charge via the Internet at <http://pubs.acs.org>.

■ AUTHOR INFORMATION

Corresponding Author

*E-mail: claudia.sissi@unipd.it, tel.: +39-049 8275711.

■ ACKNOWLEDGMENT

This work was supported by AIRC (Associazione Italiana per la Ricerca sul Cancro) grant # 5286.

■ ABBREVIATIONS:

AA, amino acid; AQ, anthraquinones; β -Ala, β -alanine; TBTU, *O*-(benzotriazol-1-yl)-*N,N,N',N'*-tetramethyluronium tetrafluoroborate; HOBT, hydroxybenzotriazole; DIPEA, diisopropylethylamine; TFA, trifluoroacetic acid; DMF, dimethylformamide; EGTA, ethylene glycol-*bis*(β -aminoethyl)-*N,N,N',N'*-tetraacetic acid; DMSO, dimethylsulfoxide; FAM, fluorescein; T_m , melting temperature; CD, circular dichroism; MTT, (3-(4,5-dimethylthiazol-2-yl)-2,5-diphenyltetrazolium; PCR, polymerase chain reaction; TRAP, telomerase repeat amplification protocol

■ REFERENCES

- (1) O'Sullivan, R. J., and Karlseder, J. (2010) Telomeres: protecting chromosomes against genome instability. *Nat. Rev. Mol. Cell Biol.* 11, 171–81.
- (2) Watson, J. D. (1972) Origin of concatemeric T7 DNA. *Nat. New Biol.* 239, 197–201.

- (3) Shay, J. W., Wright, W. E., and Werbin, H. (1991) Defining the molecular mechanisms of human cell immortalization. *Biochim. Biophys. Acta* 1072, 1–7.
- (4) Shay, J. W., and Bacchetti, S. (1997) A survey of telomerase activity in human cancer. *Eur. J. Cancer* 33, 787–91.
- (5) Greider, C. W., and Blackburn, E. H. (1985) Identification of a specific telomere terminal transferase activity in Tetrahymena extracts. *Cell* 43, 405–13.
- (6) Folini, M., Gandellini, P., and Zaffaroni, N. (2009) Targeting the telosome: therapeutic implications. *Biochim. Biophys. Acta* 1792, 309–16.
- (7) Neidle, S. (2010) Human telomeric G-quadruplex: the current status of telomeric G-quadruplexes as therapeutic targets in human cancer. *Febs J.* 277, 1118–25.
- (8) Davis, J. (2004) G-quartets 40 years later: from 5'-GMP to molecular biology and supramolecular chemistry. *Angew. Chem.* 43, 668–698.
- (9) De Cian, A., Lacroix, L., Douarre, C., Temime-Smaali, N., Trentesaux, C., Riou, J. F., and Mergny, J. L. (2008) Targeting telomeres and telomerase. *Biochimie* 90, 131–155.
- (10) Neidle, S. (2009) The structures of quadruplex nucleic acids and their drug complexes. *Curr. Opin. Struct. Biol.* 19, 239–50.
- (11) Monchaud, D., and Teulade-Fichou, M. P. (2008) A hitchhiker's guide to G-quadruplex ligands. *Org. Biomol. Chem.* 6, 627–36.
- (12) Perry, P. J., Gowan, S. M., Reszka, A. P., Polucci, P., Jenkins, T. C., Kelland, L. R., and Neidle, S. (1998) 1,4- and 2,6-disubstituted amidoanthracene-9,10-dione derivatives as inhibitors of human telomerase. *J. Med. Chem.* 41, 3253–60.
- (13) Perry, P. J., Read, M. A., Davies, R. T., Gowan, S. M., Reszka, A. P., Wood, A. A., Kelland, L. R., and Neidle, S. (1999) 2,7-Disubstituted amidofluorenone derivatives as inhibitors of human telomerase. *J. Med. Chem.* 42, 2679–84.
- (14) Perry, P. J., Reszka, A. P., Wood, A. A., Read, M. A., Gowan, S. M., Dosanjh, H. S., Trent, J. O., Jenkins, T. C., Kelland, L. R., and Neidle, S. (1998) Human telomerase inhibition by regioisomeric disubstituted amidoanthracene-9,10-diones. *J. Med. Chem.* 41, 4873–84.
- (15) Zagotto, G., Sissi, C., Lucatello, L., Pivetta, C., Cadamuro, S. A., Fox, K. R., Neidle, S., and Palumbo, M. (2008) Aminoacyl-anthraquinone conjugates as telomerase inhibitors: synthesis, biophysical and biological evaluation. *J. Med. Chem.* 51, 5566–74.
- (16) Zagotto, G., Sissi, C., Moro, S., Dal Ben, D., Parkinson, G. N., Fox, K. R., Neidle, S., and Palumbo, M. (2008) Amide bond direction modulates G-quadruplex recognition and telomerase inhibition by 2,6 and 2,7 bis-substituted anthracenedione derivatives. *Bioorg. Med. Chem.* 16, 354–61.
- (17) Dahan, A., Ashkenazi, T., Kuznetsov, V., Makievski, S., Drug, E., Fadeev, L., Bramson, M., Schokoroy, S., Rozenshine-Kemelmakher, E., and Gozin, M. (2007) Synthesis and evaluation of a pseudocyclic trithiourea-based anion host. *J. Org. Chem.* 72, 2289–96.
- (18) De Cian, A., Guittat, L., Kaiser, M., Sacca, B., Amrane, S., Bourdoncle, A., Alberti, P., Teulade-Fichou, M. P., Lacroix, L., and Mergny, J. L. (2007) Fluorescence-based melting assays for studying quadruplex ligands. *Methods* 42, 183–95.
- (19) Risitano, A., and Fox, K. R. (2003) Stability of intramolecular DNA quadruplexes: comparison with DNA duplexes. *Biochemistry* 42, 6507–13.
- (20) Crothers, D. M. (1971) Statistical thermodynamics of nucleic acid melting transitions with coupled binding equilibria. *Biopolymers* 10, 2147–60.
- (21) Darby, R. A., Sollogoub, M., McKeen, C., Brown, L., Risitano, A., Brown, N., Barton, C., Brown, T., and Fox, K. R. (2002) High throughput measurement of duplex, triplex and quadruplex melting curves using molecular beacons and a LightCycler. *Nucleic Acids Res.* 30, e39.
- (22) Ambrus, A., Chen, D., Dai, J., Bialis, T., Jones, R. A., and Yang, D. (2006) Human telomeric sequence forms a hybrid-type intramolecular G-quadruplex structure with mixed parallel/antiparallel strands in potassium solution. *Nucleic Acids Res.* 34, 2723–35.
- (23) Tanious, F. A., Jenkins, T. C., Neidle, S., and Wilson, W. D. (1992) Substituent position dictates the intercalative DNA-binding mode for anthracene-9,10-dione antitumor drugs. *Biochemistry* 31, 11632–40.
- (24) De Cian, A., Cristofari, G., Reichenbach, P., De Lemos, E., Monchaud, D., Teulade-Fichou, M. P., Shin-Ya, K., Lacroix, L., Lingner, J., and Mergny, J. L. (2007) Reevaluation of telomerase inhibition by quadruplex ligands and their mechanisms of action. *Proc. Natl. Acad. Sci. U. S. A.* 104, 17347–52.
- (25) Lown, J. W. (1993) Anthracycline and anthraquinone anticancer agents: current status and recent developments. *Pharmacol. Ther.* 60, 185–214.
- (26) Folini, M., Pivetta, C., Zagotto, G., De Marco, C., Palumbo, M., Zaffaroni, N., and Sissi, C. (2010) Remarkable interference with telomeric function by a G-quadruplex selective bisantrene regioisomer. *Biochem. Pharmacol.* 79, 1781–90.